

Metformin reduces SATB2-mediated osteosarcoma stem cell-like phenotype and tumor growth via inhibition of N-cadherin/NF- κ B signaling

H.Y. XU¹, W. FANG², Z.W. HUANG³, J.C. LU¹, Y.O. WANG¹, Q.L. TANG¹, G.H. SONG¹, Y. KANG¹, X.J. ZHU¹, C.Y. ZOU¹, H.L. YANG⁴, J.N. SHEN¹, J. WANG¹

¹Department of Musculoskeletal Oncology, the First Affiliated Hospital of Sun Yat-sen University, Guangzhou, Guangdong, China

²Department of Laboratory Medicine, Central Hospital of Huizhou, Huizhou, Guangdong, China

³Department of Orthopaedics, the Fifth Affiliated Hospital of Sun Yat-sen University, Zhuhai, China

⁴Department of Pathophysiology, Zhongshan School of Medicine, Sun Yat-sen University, Guangzhou, China

Huaiyuan Xu and Wei Fang contributed equally to this work

Abstract. – OBJECTIVE: To investigate the role of SATB2 in stem cell-like properties of osteosarcoma and identify new strategies to eliminate cancer stem cells of osteosarcoma.

MATERIALS AND METHODS: Osteosarcoma cancer stem cells were derived by sarcosphere generation or chemo drug enrichment. SATB2 and pluripotency-associated gene expression in osteosarcoma CSCs were analyzed using qRT-PCR and Western blotting. The sphere formation assay, cell counting kit-8 assay and anti-chemotherapy proteins were used to measure the effects of altered SATB2, N-cadherin expression or metformin treatment in CSCs. Nude mice were injected with SATB2-deficient U2OS/MTX cells to assess the role of SATB2 in osteosarcoma growth and chemoresistance *in vivo*. Bioinformatics analyses were performed to identify SATB2 downstream target genes and immunohistochemistry to determine the correlation between SATB2 expression and patient outcome. Western blotting and luciferase reporter assays were used to examine the effects of N-cadherin and SATB2 inhibition on the NF- κ B pathway.

RESULTS: SATB2 was upregulated in osteosarcoma stem cells. Knockdown of SATB2 decreased sarcosphere formation, cell proliferation and stem cell-like gene expression *in vitro*, meanwhile reduced tumor growth and chemoresistance *in vivo*. High SATB2 expression in osteosarcoma patient samples was associated with poor clinical outcome. N-cadherin was one critical downstream target gene of SATB2 that mediated the stem cell-like phenotype. Reduction of SATB2 or N-cadherin resulted in NF- κ B inactivation, which led to impaired osteosarcoma

sphere formation and tumor cell proliferation. Metformin treatment of osteosarcoma cells enhanced the effects of chemotherapy via suppression of N-cadherin.

CONCLUSIONS: SATB2 plays an important role in regulating osteosarcoma stem cell-like properties and tumor growth. The combination of conventional chemotherapy and metformin may be a promising therapeutic strategy for osteosarcoma patients.

Key Words:

Cancer stem cells, Chemoresistance, Metformin, N-cadherin, Osteosarcoma, SATB2, Tumorigenesis.

Abbreviations

OS = osteosarcoma; CSCs = cancer stem cells, MTX = methotrexate; DOX = doxorubicin.

Introduction

Osteosarcoma (OS) is the most common type of bone-forming malignant mesenchymal tumor and is characterized by intrinsic therapeutic resistance¹. Therapeutic failure may occur because of an inability to eradicate resistant subpopulations of cancer cells, which may include cancer stem cells (CSCs)^{2,3}. Recent studies have shown that dysregulation of genes or signaling pathways involved in CSC develop-

ment⁴⁻⁹. Therefore, investigation of bone development regulator may help to identify new strategies to eliminate CSCs might enhance the control of OS.

Special AT-rich sequence-binding protein 2 (SATB2) is a DNA-binding protein that acts as a molecular node in the bone development transcriptional network. SATB2 knockout mice display dysregulation of skeletogenesis due to the downregulation of downstream target genes, such as RUNX2 and ATF4¹⁰. In addition to having important roles in skeletal formation, SATB2 has been shown to have significant roles in cancer biology. For example, SATB2 modulates stemness and carcinogenesis in pancreatic cancer¹¹. In head and neck squamous cell carcinoma, overexpression of SATB2 augments Δ Np63 α activity to promote chemoresistance¹². However, despite its potential functions in tumorigenic and bone development, the regulatory effects of SATB2 in OS CSCs have rarely been examined.

CDH2 (hereafter referred to as N-cadherin) encodes a transmembrane protein, N-cadherin, which is involved in cartilage development, epithelial-to-mesenchymal transition (EMT) and cancer stem/progenitor cell-like properties¹³⁻¹⁵. The intracellular domain of N-cadherin interacts with many key signaling molecules, such as NF- κ B subunit p65 and its downstream molecules^{16,17}. Excessive expression of mesenchymal N-cadherin generates cells with stem cell properties¹⁸ and leads to drastic changes in the cytoskeleton and in signaling transduction¹⁹, which ultimately promotes the development of cancers such as breast cancer, pancreatic cancer, and prostate cancer²⁰⁻²³. Additionally, N-cadherin, as a cell surface protein, is a potential drug target. For example, targeting N-cadherin effectively reduces the therapeutic resistance and metastasis of prostate cancer and breast cancer both *in vitro* and *in vivo*^{24,25}. However, the molecular mechanisms and therapeutic value of N-cadherin in OS CSCs are not fully understood.

In this investigation, we demonstrated that SATB2 acts as a potent mediator of OS stem cell-like characteristics and showed the genes and pathways downstream of SATB2. Moreover, we identified a novel and feasible approach to eliminate OS CSCs by a combination of conventional chemotherapy drugs and metformin, which might enhance the control of osteosarcoma.

Materials and Methods

Cell Lines, Reagents and Culture Conditions

The human OS cell lines U2OS/MTX used in this study were donated by Dr. M. Serra (Istituti Ortopedici Rizzoli, Bologna, Italy) and were continuously cultured in the presence of 300 μ g/L methotrexate (MTX). MTX, doxorubicin (DOX) and metformin were purchased from Sigma-Aldrich (St. Louis, MO, USA). The ZOS and ZOSM cells lines, which were obtained from a primary tumor and skipped metastasis, respectively, of an OS patient, were established at our institution²⁷. All other cell lines were purchased from the American Type Culture Collection (ATCC, Manassas, VA, USA) and cultured according to the conditions suggested by ATCC. This study was approved by the Ethics Committee of Sun Yat-sen University, and written informed consent was obtained from the patients or their guardians before sample collection. All of the animal studies were approved by the Institutional Animal Care and Use Committee (IACUC) of Sun Yat-sen University.

Sarcosphere Formation Assay

Sarcosphere formation assays were performed as previously described⁵. These experiments were performed in triplicate.

Real-time PCR

Total RNA from OS cell lines was purified using TRIzol (Invitrogen, Carlsbad, CA, USA) according to the product instructions, and first strand cDNA was synthesized using a First Strand cDNA Synthesis Kit (Fermentas, Glen Burnie, MD, USA) following the manufacturer's protocol. Real-time q-PCR was performed using SYBR® qPCR Mix (Toyobo, Osaka, Japan) according to the manufacturer's protocol and a LightCycler® 480 System. The experiments were performed in triplicate. The sequences of the primers used for the PCR are listed in Supplementary Table II.

Western Blotting

Western blotting was performed using standard procedures. The antibodies used are listed below. Pixel density was quantified using Quantity One software (Bio-Rad, Hercules, CA, USA). Antibodies against SATB2 (1:1000, EPNCIR130A, Abcam, Cambridge, MA, USA), N-cadherin (1:1000, 13769-1-AP, ProteinTech, Chicago, IL, USA), MDR1 (1:1000, #13342, Cell Signaling Technology, Danvers, MA, USA), PARP (1:1000, ab194586, Abcam, Cambridge, MA, USA) and GAPDH

(1:10000, ab128915, Abca, Cambridge, MA, USA) were used.

Cell Counting kit-8 Assay (CCK-8)

OS cells (100 μ L) were seeded at a density of 2,000 cells/well in 96-well plates. After incubation for 24, 48, 72, 96 and 120 h, CCK-8 solution (10 μ L, Beyotime, Shanghai, China) was added to the wells. The plates were incubated for additional 2 h, and absorbance was measured at 450 nm. The experiments were performed in triplicate.

In Vivo Animal Models

All animal studies were performed in accordance with the principles and procedures outlined in the guidelines of the Institutional Animal Care and Use Committee at Sun Yat-sen University. Female nude mice were purchased from Guangdong Medical Laboratory Animal Centre (Foshan, China). To develop the orthotopic OS model, the mice were anesthetized with 4% chloral hydrate (100 g/0.2 mL) by intraperitoneal injection. Then, sh.SATB2 and sh.Ctrl U2OS/MTX cells (2×10^6) were implanted into the proximal tibia of the mice (n=10 per group). On the 7th day, each group of mice was randomly divided into 2 subgroups (n=5 per group), and phosphate buffered saline (PBS) or MTX (0.4 mg/kg body weight) was intraperitoneally injected into the mice once a week. The mice were monitored three times weekly. Tumor volume was calculated using the formula $V = 4/3\pi [1/4(D1+D2)]^2$. When tumor lengths exceeded 1.5 cm, the experiment was stopped, and the mice were sacrificed by cervical dislocation.

Luciferase Reporter Assays

Cells were seeded at 4×10^4 cells/well in 24-well plates and co-transfected with an N-cadherin promoter (GeneCopoeia, Rockville, MD USA) or NF- κ B p65 luciferase reporters (Genomeditech, Shanghai, China) and pRL-TK plasmid (Promega, Madison, WI, USA) using Lipofectamine 3000 (Invitrogen, Carlsbad, CA, USA). After 48 h, the cells were harvested in passive lysis buffer (PLB) (Promega, Madison, WI, USA), and luciferase activity was measured using the Dual-Luciferase Reporter Assay System (Promega, Madison, WI, USA) on a GloMax Luminometer (Promega, Madison, WI, USA).

Statistical Analysis

All of the statistical analyses were performed using SPSS (version 16.0) software (SPSS Inc.,

Chicago, IL, USA). The data were analyzed using the Student's t-test. Survival curves were calculated using the Kaplan-Meier method, and differences were analyzed using the log-rank test. *p*-values less than 0.05 were considered significant.

Experimental Procedures

See the Supplemental Methods for details on other experimental procedures.

Results

SATB2 Expression is Elevated in OS CSCs and is Associated with Poor Outcome

OS CSCs can be enriched by either sarco-sphere selection or chemotherapeutic agent selection^{5,6}. To examine SATB2 expression in osteosarcoma CSCs, we first isolated sarco-spheres from 143B, U2OS/MTX, and U2OS cells and then returned them to adherent culture (Figure 1A). The sarco-spheres expressed elevated levels of SATB2 and other genes that are associated with a stem cell-like phenotype, including SOX2, OCT3/4, and CD133. These elevated levels were lost upon redifferentiation (Figure 1B). Likewise, after doxorubicin-induced CSC enrichment, we also observed elevated SATB2 expression in these cell subpopulations (Figure 1C). In patient samples, SATB2 expression was significantly higher in OS tissues than in skeletal muscle according to the analysis of publicly available datasets (GSE14827 and GSE6798)²⁶⁻²⁸ ($p < 0.0001$, Figure 1D). Moreover, we assessed the clinical relevance of SATB2 in OS samples that were obtained from our hospital using immunohistochemistry and in a public dataset (GSE21257) using a bioinformatics method²⁹. The characteristics of the patients with OS are listed in Table I. We found that elevated SATB2 expression was associated with a lower survival rate and a lower lung metastasis-free survival rate (Figure 1E, F, and Figure S1A). Besides, we found that SATB2 DNA copy number amplification was followed by mRNA upregulation in 265 sarcoma patient samples from TCGA database (Figure S1B), which indicates that SATB2 ectopic expression in OS is linked to DNA copy alteration. Accordingly, these data indicate that elevated SATB2 levels may contribute to OS stem cell-like properties and were correlated with a poorer outcome in OS patients.

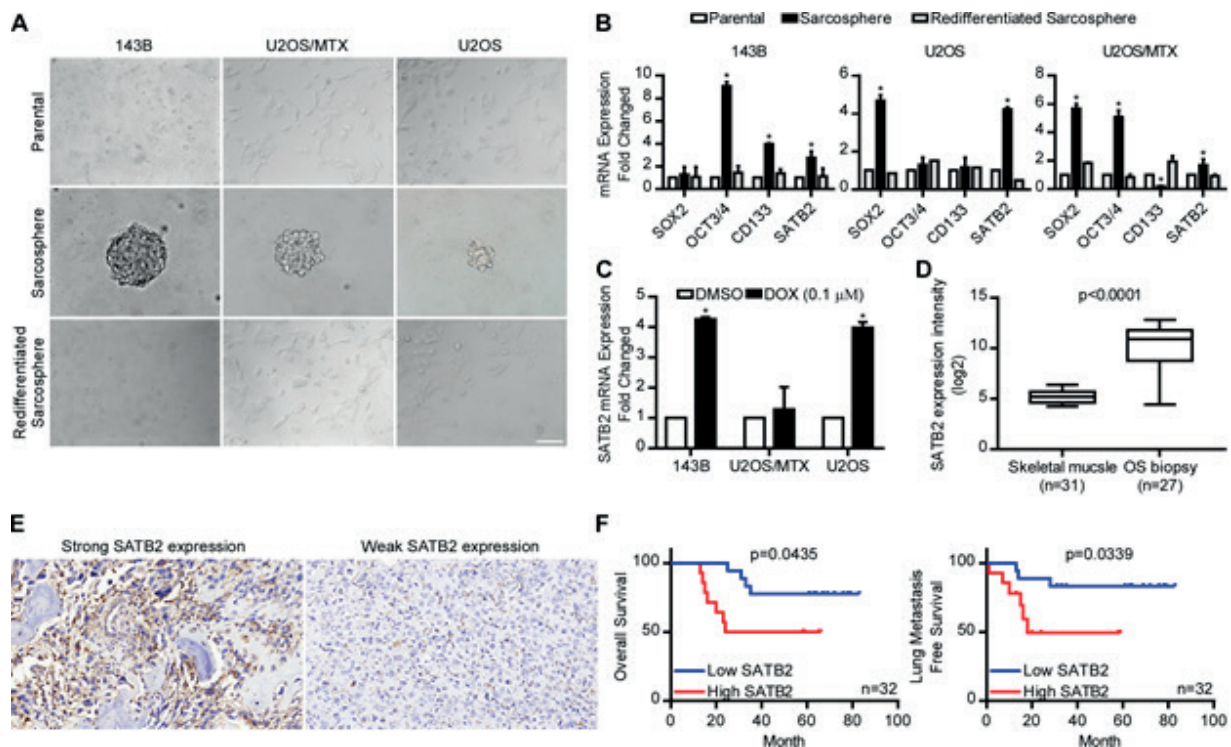


Figure 1. SATB2 expression is elevated in OS CSCs and is associated with poor outcome. (A) U2OS/MTX, 143B, and U2OS parental adherent cells (top), sarcospheres in low-adherence cultures (middle), and re-differentiated sarcosphere cells after return to adherent cultures (bottom). Scale bar, 100 μ m. (B) qPCR results for putative stem cell markers and SATB2 mRNA expressed as a fold-change relative to parental cells \pm SEM (n=3, * p <0.05, two-tailed Student's t-test). (C) SATB2 mRNA expression in OS cell lines after dimethyl sulfoxide (DMSO) or DOX (0.1 μ M for 3 days) treatment quantified by qPCR. (D) SATB2 expression in normal skeletal muscle (GSE13205) and biopsy samples (GSE14827) detected using an Affymetrix Human Genome U133 Plus 2.0 Array. Data are presented as box-plots. (E) Representative images of weak and strong SATB2 expression in the samples. (F) Overall survival rate was significantly higher in the low SATB2 expression group than in the high expression group, as indicated by Kaplan-Meier analysis (log-rank test, p =0.0435). The risk of lung metastasis was higher in the high SATB2 expression group (log-rank test, p =0.0339).

Knockdown of SATB2 Attenuates Stem Cell-like Properties and Tumor Growth in OS

To test whether SATB2 regulates OS CSCs, we first knocked down SATB2 using two different sh.SATB2 constructs or upregulated its expression level in OS cells (Figure S2A). Interestingly, SATB2-deficient 143B cells switched from a fibroblast-like phenotype to a cuboidal phenotype, indicating that mesenchymal properties were lost and epithelial characteristics were acquired (Figure S2B). Next, we determined the effects of SATB2 on stem cell-like characteristics. We found that knockdown of SATB2 showed lower sphere formation number and stem-associated genes expression level in 143B and U2OS/MTX whereas these phenotypes were increased after SATB2 was overexpressed in U2OS cells (Figure 2A-C). Moreover, reduced SATB2 expression inhibited cell proliferation (Figure 2D), indicating that inhi-

bition of SATB2 suppresses the tumor-initiating potential of tumor cells. Another important property of CSCs is resistance to chemotherapy, and this phenotype is primarily mediated by ATP-binding cassette transporters, such as multidrug-resistant protein (MDR1)³⁰. We found that SATB2-deficient U2OS/MTX cells showed weaker anti-chemotherapeutic phenotypes, as indicated by the downregulation of MDR1 and upregulation of the apoptosis-related protein PARP (Figure 2E). By contrast, SATB2 restoration in U2OS cells enhanced cell growth and chemotherapy resistance (Figure 2D and E). Furthermore, we assessed the role of SATB2 in OS stem cell-like features using mouse models. We implanted sh.SATB2 or sh.Ctrl U2OS/MTX cells (2×10^6) into the proximal tibia of the mice (n=10 per group). On the 7th day, each group of mice was randomly divided into 2 subgroups (n=5 per group), and PBS or MTX (0.4 mg/kg body weight) was intra-

Table I. Clinical characteristics of the 32 OS patients.

	Percentage (%)	Number	SATB2 expression	
			High	Low
Age (years)				
0-20	75.00	24	10	14
21-40	21.88	7	4	3
41-100	3.13	1	0	1
Gender				
Male	65.63	21	9	12
Female	34.38	11	5	6
Location				
Distal femur	43.75	14	6	8
Proximal tibia	25.00	8	3	5
Proximal humerus	21.88	7	4	3
Proximal femur	6.25	2	1	1
Other	3.13	1	0	1
Enneking				
IIB	90.63	29	16	13
III	9.38	3	2	1
Relapse				
Yes	9.38	3	0	3
No	90.63	29	14	15
Lung metastasis				
Yes	28.13	9	6	3
No	71.88	23	8	15
Death				
Yes	34.38	11	7	4
No	65.63	21	7	14

peritoneally injected into the mice once a week. By day 32, we observed that the SATB2-deficient group exhibited a significant reduction in tumor growth rate and a striking synergistic effect with MTX treatment (Figure 2F-H). Thus, our results suggest that inhibition of SATB2 suppressed the tumor-initiating stem-like features of OS.

SATB2 Enhances OS Stem Cell-Like Characteristics Through the Induction of N-cadherin/NF- κ B signaling

To investigate the genes and pathways downstream of SATB2 that function to promote OS, we performed bioinformatics screening utilized a SATB2 ChIP-seq dataset (SRX1028899)³¹ and

gene expression data (GSE21257) from OS biopsy samples²⁹, from which we selected 21 candidates (Figure 3A and Table II). According to gene ontology (GO) analysis, all 21 genes clustered with biomineral tissue development, ossification, and bone mineralization. This clustering was consistent with the role of SATB2 in regulating skeletal development (Table SI), which further confirmed the reliability of our screening procedure. We were particularly interested in N-cadherin (CDH2) due to its significant positive correlation with SATB2 ($r=0.723$, $p<0.0001$) (Figure S3A) and its crucial role in EMT, stem cell-like properties, and tumor progression^{15,16,25}. We wonder if SATB2 play an important role in N-cadhe-

Table II. Binary logistic regression analysis.

Characteristics	Odds Ratio (95% CI)	p-value
Age (year)	1.11 (0.97 to 1.26)	0.12
Male gender (%)	3.01 (0.70 to 13.35)	0.14
BMI (kg/m ²)	1.16 (0.73 to 1.84)	0.52
Left atrial diameter (mm)	1.43 (1.18 to 1.73)	<0.01
UCP-1 mRNA in SAT	0.66 (0.43 to 1.00)	0.50
UCP-1 mRNA in PAT	0.85 (0.74 to 0.98)	0.03
UCP-1 mRNA in EAT	0.71 (0.52 to 0.96)	0.03

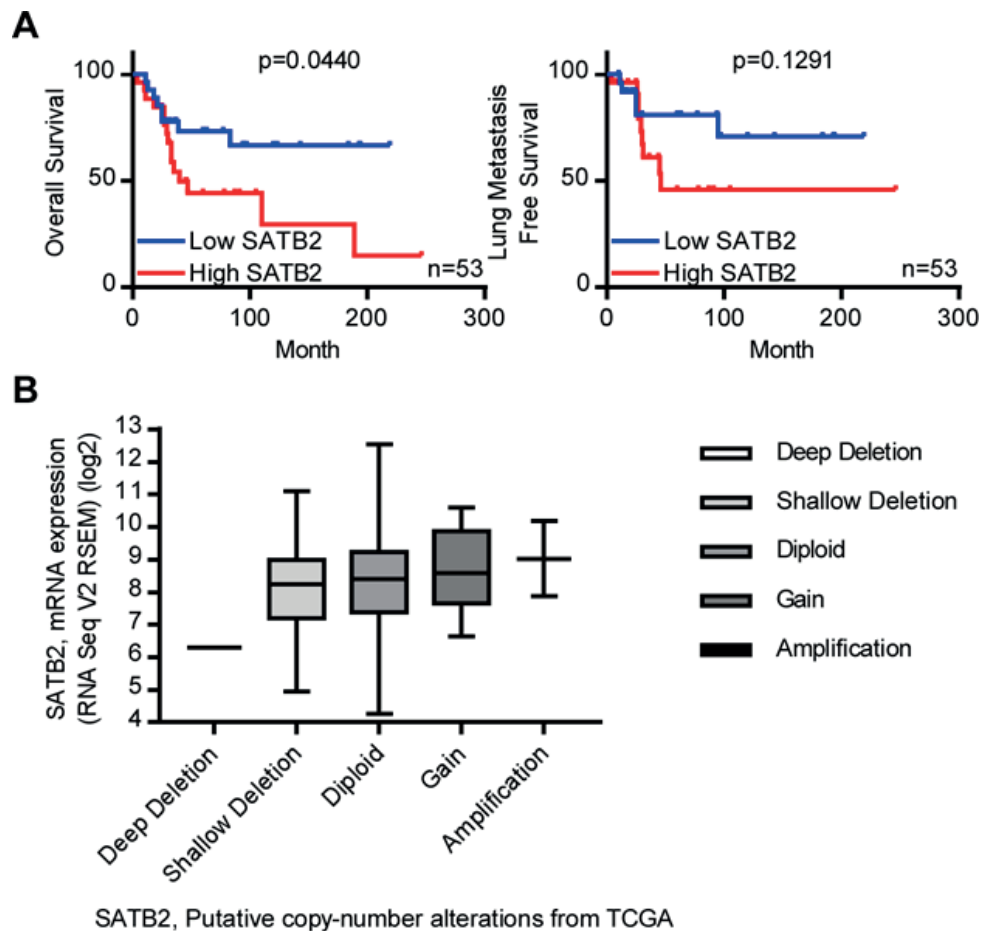


Figure S1. (A) Samples with high SATB2 expression were correlated with worse overall survival (log-rank test, $p=0.0440$). The risk of lung metastasis was higher in the low SATB2 expression group than that in the high expression group, although this difference was not significant (log-rank test, $p=0.1291$). (B) SATB2 mRNA expression data and copy number alteration data of 265 sarcoma patients from TCGA database are presented as box-plots.

rin expression regulation. After SATB2 shRNA transfection, we found that whether the mRNA level, protein levels or the promoter luciferase reporter activity of N-cadherin were downregulated while upregulated by SATB2 overexpression (Figure 3B, E and Figure S3B). Moreover, knockdown of N-cadherin reversed sarcosphere formation and cell proliferation in U2OS-SATB2 cells (Figure 3C and D), indicating that N-cadherin is required for the SATB2-mediated features of CSCs. As N-cadherin lies upstream of the NF- κ B pathway, and activation of NF- κ B is essential for OS progression^{16,32-35}, we hypothesized that the sequential activation of SATB2, N-cadherin, and NF- κ B contributes to OS CSC development. As expected, knockdown of SATB2 alleviated I κ B α phosphorylation and NF- κ B p65 nuclear translocation, concomitant with a substantial reduction

in NF- κ B luciferase reporter activity in both 143B and U2OS/MTX cells. In contrast, overexpression of SATB2 in U2OS cells increased NF- κ B p65 nuclear accumulation, phosphorylation of I κ B α , and NF- κ B luciferase reporter activity. These effects were reversed by knockdown of N-cadherin in U2OS-SATB2 cells (Figure 3E-F). Hence, our results support an essential role for N-cadherin/NF- κ B signaling in OS CSCs.

Metformin Inhibits OS CSC Traits

Considering that N-cadherin induction is an essential step in SATB2-mediated tumor malignancy and that N-cadherin can be repressed by metformin¹⁶, we wonder whether pharmacologic inhibition of N-cadherin recapitulates the effects of N-cadherin or SATB2 inhibition. To this end, we treated 143B cells with incre-

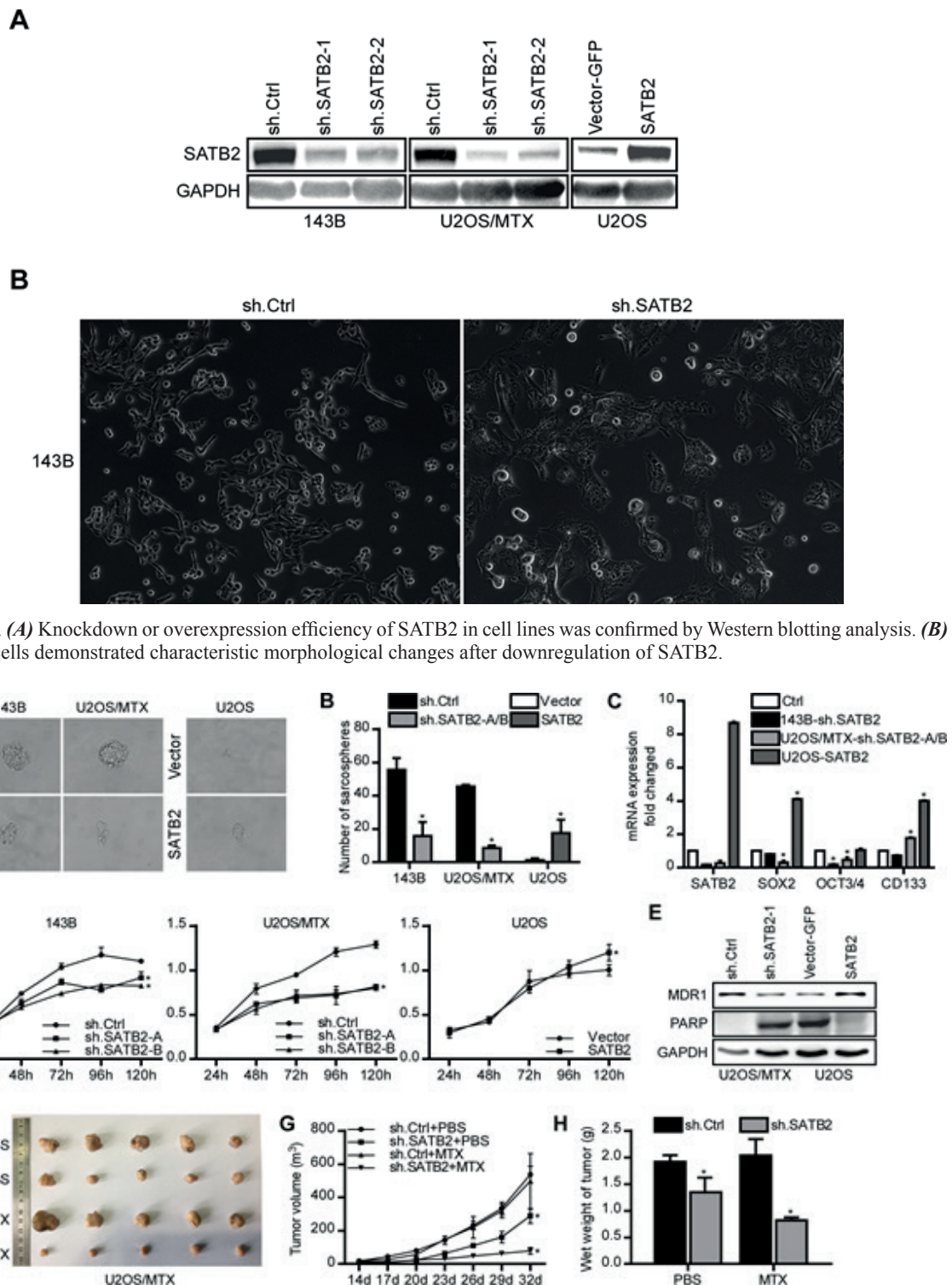


Figure 2. Knockdown of SATB2 attenuates stem-like properties and tumor growth. **(A-B)** Sarcosphere formation assays were performed in the indicated cells. **(C)** The mRNA expression of stem cell markers was examined by qPCR after knockdown or overexpression of SATB2 in cell lines. **(D)** Cell proliferation in 143B, U2OS/MTX, and U2OS cells was determined using CCK-8 assays after knockdown or overexpression of SATB2. **(E)** MDR1 and PARP levels were measured using Western blotting analyses in cells following MTX treatment (300 $\mu\text{g/L}$ for 24 h). **(F-H)** An orthotopic model was used to assess the effects of SATB2 on the growth and chemoresistance of U2OS/MTX cells *in vivo*. Mice were monitored three times weekly. All *in vitro* experiments were repeated at least 3 times. Mean values and standard deviations were calculated (* $p < 0.05$, two-tailed Student's *t*-test).

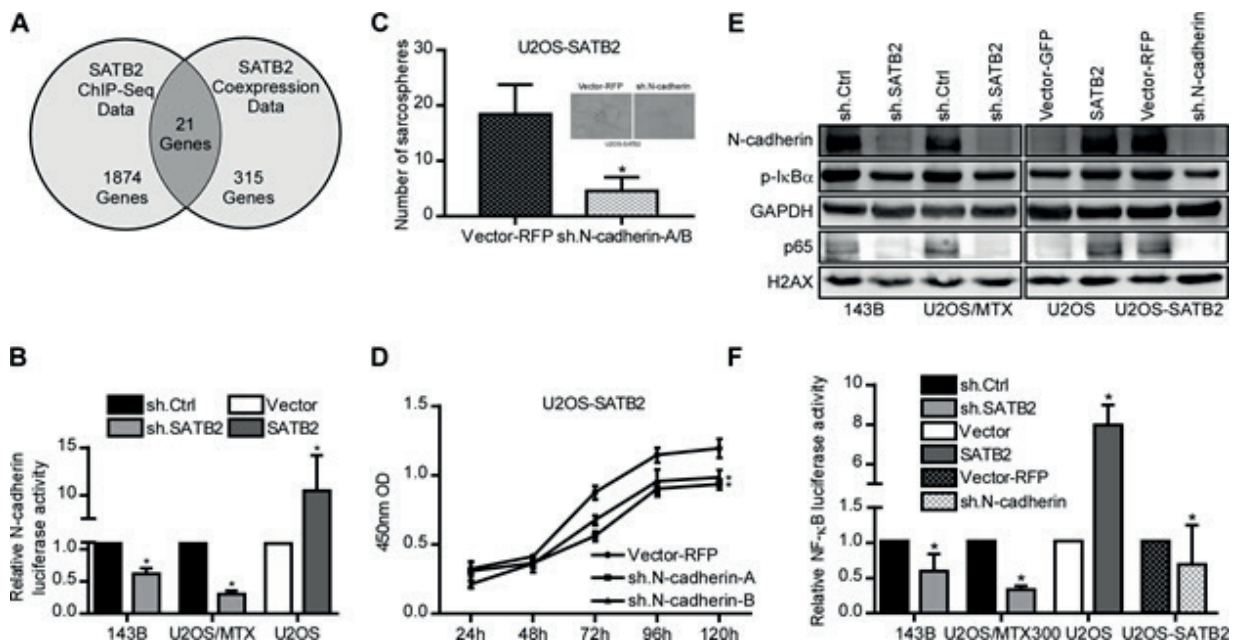


Figure 3. SATB2 enhances OS stem-like characteristics through induction of N-cadherin/NF-κB signaling. *(A)* A combination of SATB2 ChIP-seq data and co-expression data were used to identify genes that are directly targeted by SATB2. *(B)* N-cadherin promoter luciferase reporter constructs were transiently transfected into the indicated cells, and luciferase activity was analyzed after 48 h. *(C-D)* N-cadherin knockdown decreased spheroid formation and cell growth in SATB2-overexpressing U2OS cells. *(E)* Lysates from the indicated cells were immune-blotted for N-cadherin, phosphorylated IκBα, and NF-κB p65. *(F)* NF-κB luciferase reporter assays were performed on the indicated cells.

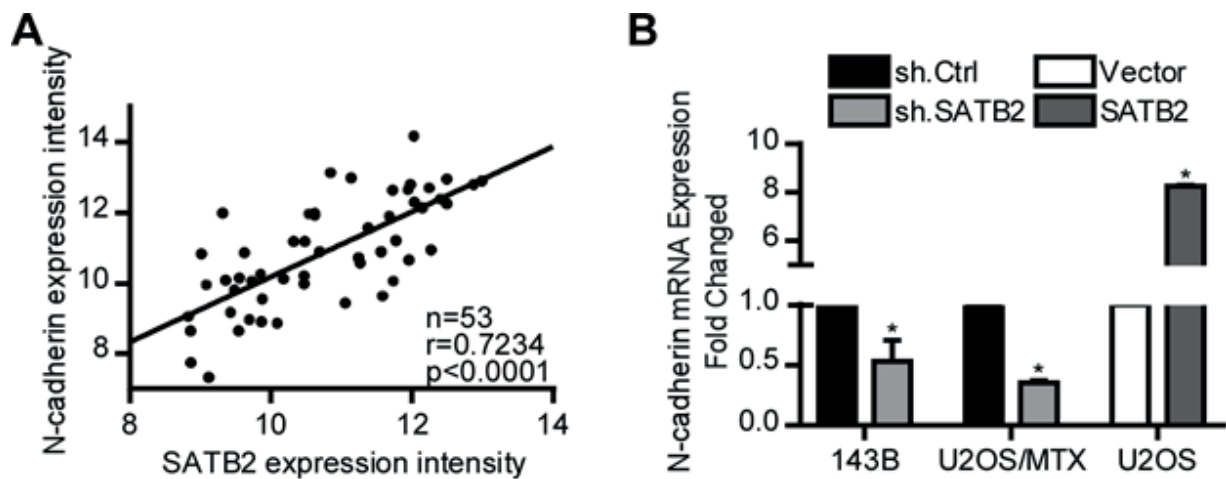


Figure S3. *(A)* The expression association of SATB2 and N-cadherin in tissues ($n=53$) was examined in GSE21257. *(B)* N-cadherin mRNA levels in the indicated cells were determined by Western blotting and qPCR analyses. $*p<0.05$ according to the two-tailed Student's *t*-test.

using amount of metformin (0, 10, 20, and 40 mM). Consequently, we found that treatment with metformin reduced N-cadherin protein levels as well as the formation of spheroids number in a dose-dependent manner (Figure 4A-

B). To identify whether treatment of metformin recapitulates the anti-chemoresistance effects of SATB2 inhibition, we combined use with MTX and metformin in U2OS/MTX cells. As expected, the treatment induced increased che-

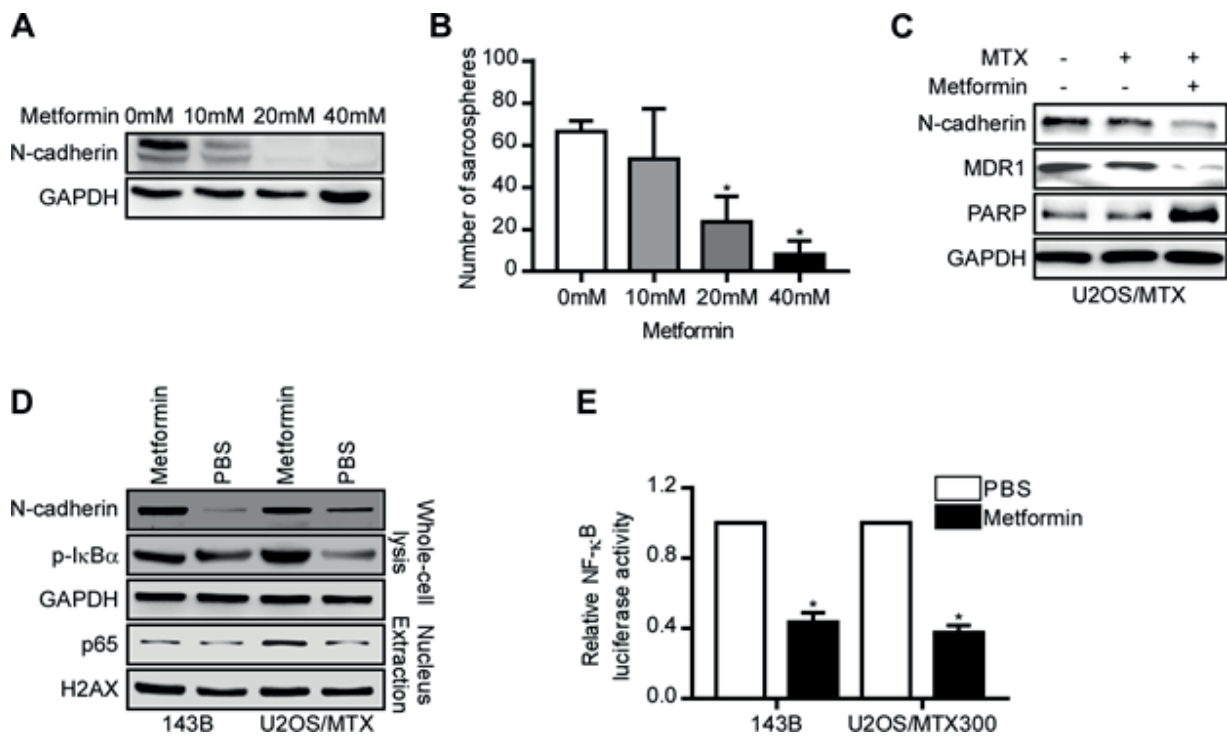


Figure 4. Metformin inhibits OS CSCs traits. (A-B) OS cells were exposed to increasing doses of metformin (0, 10, 20, and 40 mM), N-cadherin expression was detected by Western blotting and sarcosphere formation capacity was measured. Experiments were repeated at least 3 times. Mean values and standard deviations were calculated. * $p < 0.05$ according to two-tailed Student's *t*-test. (C) N-cadherin, MDR1, and PARP protein levels were measured by Western blot analyses following a combination of MTX and metformin treatment (10 mM for 24 h). (D-E) The effects of metformin on the NF- κ B pathway were confirmed by Western blotting analysis and luciferase reporter assays.

mosensitivity and cell apoptosis, as shown by the upregulation of MDR1 and PARP (Figure 4C). Further, to clarify the underlying mechanisms of metformin therapy, we exposed U2OS/MTX cells to metformin (10 mM) alone. We found that the use of metformin results in the suppression of N-cadherin expression, NF- κ B p65 nuclear accumulation, and NF- κ B luciferase reporter activity (Figure 4D and E). Accordingly, our findings demonstrate the efficacy of combined metformin and traditional chemotherapy drugs for treating refractory OS.

Discussion

Accumulating evidence supports the existence of tumor-initiating or CSCs in OS. Subpopulations of these cells are responsible for tumor maintenance, chemotherapy resistance, relapse, and metastasis^{5,36,37}. SATB2 has been found to regulate skeletal development¹⁰ and shows a very high immun-expression rate in bone tumor samples, reaching 90.4-100%³⁸⁻⁴⁰. We hypothesized that SATB2

might be involved in modulating OS CSCs. Here, we found that SATB2 was upregulated in OS stem cells. Knockdown of SATB2 abrogated OS stem cell-like properties *in vitro*, as evidenced by the reduction of sarcosphere formation, cell proliferation and associated stem cell-like gene expression. SATB2 deficiency also led to reductions in the tumor growth rate and anti-drug capacity in our mouse orthotopic model. We also found that clinical samples from OS patients showed a positive correlation between high SATB2 expression and poor patient outcome. Besides, SATB2 has recently been found to promote OS migration *in vitro*⁴¹ and to correlate positively with the degree of chondrosarcoma malignancy⁴⁰; these findings further support our hypothesis. Nevertheless, clinical translation is limited because SATB2 is neither a targetable cell surface protein nor a druggable enzyme. Therefore, research of SATB2 targeted therapy is still needed and targeting downstream pathways or genes that are mediated by the overproduction of SATB2 may be an alternative therapeutic strategy.

Using bioinformatics analysis, we identified N-cadherin (CDH2) as a downstream target gene

of SATB2. Recently, increasing N-cadherin accumulation is believed to generate tumor cells with stem-like properties^{18,42}. In our research, we showed that SATB2 upregulates N-cadherin transcriptional activity and expression level. The inhibition of N-cadherin reversed the increase in sarcosphere-forming ability induced by SATB2 overexpression. These results partially explain why SATB2 modulates stemness and carcinogenesis. Furthermore, N-cadherin is a signal transduction molecule of the upstream protein NF- κ B^{16,32}. Our results demonstrated that the reduction of either SATB2 or N-cadherin leads to NF- κ B inactivation and the impairment of OS sarcosphere formation and tumor cell proliferation, suggesting an anti-tumor role of NF- κ B targeted therapy. Although other SATB2 regulatory genes or pathway exist in OS progression, our result provides, at least at one aspect, show that N-cadherin/NF- κ B pathway inhibition might be an effective means of suppressing stem cell-like properties in OS cells.

Considering the tumor-promoting role of SATB2 and N-cadherin in OS, clinical use of the cell surface protein N-cadherin, rather than SATB2, is more feasible for pharmaceutical targeting. Clinical trials using N-cadherin antagonists, such as ADH-1, resulted in significantly better outcomes of melanoma patients⁴³. However, OS is predominantly found in children and adolescents, and the toxicity and safety of a targeting drug in these populations have not yet been assessed. Metformin is one of the most commonly prescribed oral anti-diabetic drugs worldwide. Emerging evidence indicates that metformin has an anti-cancer effect. For instance, in prostate cancer, metformin regulates NF- κ B signaling by inhibiting N-cadherin¹⁶. Jiralerspong et al⁴⁴ reported that diabetic patients with breast cancer who received metformin and neoadjuvant chemotherapy showed 16% higher pathologic complete response than did diabetics who did not receive metformin. We found that the inhibition of N-cadherin by metformin recapitulates the effects of N-cadherin or SATB2 inhibition, resulting in the suppression of the stem cell-like phenotype and NF- κ B activation. Accordingly, metformin is a promising solution for safely targeting SATB2 downstream pathways and genes, but further research is required.

Conclusions

SATB2 enhances the stem cell-like traits, tumor growth and chemoresistance of OS through induction of the N-cadherin/NF- κ B signaling

pathway. The combination of conventional chemotherapy and metformin may represent a promising therapeutic intervention for OS patients.

Acknowledgments

We thank Yujie Cai (the First Affiliated Hospital of Sun Yat-sen University) and Yixiang Xu (Geneseeq Technology Inc.) for expert technical assistance.

Funding

This research was supported by the National Natural Science Foundation of China 81272940, 81472507 to Jin Wang; the Science and Technology Program of Guangzhou 201504291231256 to Jin Wang; the Sun Yat-sen University Clinical Research 5010 Program 2012002, to Jin Wang; and the Ph.D. program foundation of the Ministry of Education of China (20130171110062 to Jin Wang). The funders had no role in the study design, data collection and analysis, decision to publish, or preparation of the manuscript.

Conflict of interest

The authors declare that they have no competing interests.

References

- BIERMANN JS, ADKINS D, BENJAMIN R, BRIGMAN B, CHOW W, CONRAD EU, FRASSICA D, FRASSICA FJ, GEORGE S, HEALEY JH, HECK R, LETSON GD, MAYERSON J, MCGARRY SV, O'DONNELL RJ, PATT J, RANDALL RL, SANTANA V, SATCHER RL, SCHMIDT RG, SIEGEL HJ, WONG MK, YASKO AW, National Comprehensive Cancer Network. Bone cancer. *J Natl Compr Canc Netw* 2007; 5: 420-437.
- REYA T, MORRISON SJ, CLARKE MF, WEISSMAN IL. Stem cells, cancer, and cancer stem cells. *Nature* 2001; 414: 105-111.
- AL-HAJJ M, CLARKE MF. Self-renewal and solid tumor stem cells. *Oncogene* 2004; 23: 7274-7282.
- RAJASEKHAR VK, STUDER L, GERALD W, SOCCI ND, SCHER HI. Tumour-initiating stem-like cells in human prostate cancer exhibit increased NF- κ B signalling. *Nat Commun* 2011; 2: 162.
- TANG QL, ZHAO ZQ, LI JC, LIANG Y, YIN JQ, ZOU CY, XIE XB, ZENG YX, SHEN JN, KANG T, WANG J. Salinomycin inhibits osteosarcoma by targeting its tumor stem cells. *Cancer Lett* 2011; 311: 113-121.
- LU J, SONG G, TANG Q, YIN J, ZOU C, ZHAO Z, XIE X, XU H, HUANG G, WANG J, LEE DF, KHOKHA R, YANG H, SHEN J. MiR-26a inhibits stem cell-like phenotype and tumor growth of osteosarcoma by targeting Jagged1. *Oncogene* 2017; 36: 231-241.
- RODRIGUEZ R, RUBIO R, MENENDEZ P. Modeling sarcomagenesis using multipotent mesenchymal stem cells. *Cell Res* 2012; 22: 62-77.

- 8) MUTSAERS AJ, WALKLEY CR. Cells of origin in osteosarcoma: mesenchymal stem cells or osteoblast committed cells? *Bone* 2014; 62: 56-63.
- 9) XIAO W, MOHSENY AB, HOGENDOORN PC, CLETON-JANSEN AM. Mesenchymal stem cell transformation and sarcoma genesis. *Clin Sarcoma Res* 2013; 3: 10.
- 10) DOBREVA G, CHAHROUR M, DAUTZENBERG M, CHIRIVELLA L, KANZLER B, FARIÑAS I, KARSENTY G, GROSSCHEDL R. SATB2 is a multifunctional determinant of craniofacial patterning and osteoblast differentiation. *Cell* 2006; 125: 971-986.
- 11) YU W, MA Y, SHANKAR S, SRIVASTAVA RK. Role of SATB2 in human pancreatic cancer: implications in transformation and a promising biomarker. *Oncotarget* 2016; 7: 57783-57797.
- 12) CHUNG J, LAU J, CHENG LS, GRANT RI, ROBINSON F, KETELA T, REIS PP, ROCHE O, KAMEL-REID S, MOFFAT J, OHH M, PEREZ-ORDONEZ B, KAPLAN DR, IRWIN MS. SATB2 augments $\Delta Np63\alpha$ in head and neck squamous cell carcinoma. *EMBO Rep* 2010; 11: 777-783.
- 13) TULI R, TULI S, NANDI S, HUANG X, MANNER PA, HOZACK WJ, DANIELSON KG, HALL DJ, TUAN RS. Transforming growth factor-beta-mediated chondrogenesis of human mesenchymal progenitor cells involves N-cadherin and mitogen-activated protein kinase and Wnt signaling cross-talk. *J Biol Chem* 2003; 278: 41227-41236.
- 14) GUNTUR AR, ROSEN CJ, NASKI MC. N-cadherin adherens junctions mediate osteogenesis through PI3K signaling. *Bone* 2012; 50: 54-62.
- 15) QIAN X, ANZOVINO A, KIM S, SUYAMA K, YAO J, HULIT J, AGIOSTRATIDOU G, CHANDIRAMANI N, McDAID HM, NAGI C, COHEN HW, PHILLIPS GR, NORTON L, HAZAN RB. N-cadherin/FGFR promotes metastasis through epithelial-to-mesenchymal transition and stem/progenitor cell-like properties. *Oncogene* 2014; 33: 3411-3421.
- 16) GE R, WANG Z, WU S, ZHUO Y, OTSETOV AG, CAI C, ZHONG W, WU CL, OLUMI AF. Metformin represses cancer cells via alternate pathways in N-cadherin expressing vs. N-cadherin deficient cells. *Oncotarget* 2015; 6: 28973-28987.
- 17) SHIMOMURA T, KONO E, TRAN CP, YAMASHIRO J, WAINBERG ZA, REITER RE. N-cadherin monoclonal antibody as a therapeutic agent against chemoresistance in prostate cancer. *Cancer Res* 2011; 71: 5052-5052.
- 18) MANI SA, GUO W, LIAO MJ, EATON EN, AYYANAN A, ZHOU AY, BROOKS M, REINHARD F, ZHANG CC, SHIPITSIN M, CAMPBELL LL, POLYAK K, BRISKEN C, YANG J, WEINBERG RA. The epithelial-mesenchymal transition generates cells with properties of stem cells. *Cell* 2008; 133: 704-715.
- 19) YILMAZ M, CHRISTOFORI G. EMT, the cytoskeleton, and cancer cell invasion. *Cancer Metastasis Rev* 2009; 28: 15-33.
- 20) CAI J, GUAN H, FANG L, YANG Y, ZHU X, YUAN J, WU J, LI M. MicroRNA-374a activates Wnt/ β -catenin signaling to promote breast cancer metastasis. *J Clin Invest* 2013; 123: 566-579.
- 21) HAZAN RB, PHILLIPS GR, QIAO RF, NORTON L, AARONSON SA. Exogenous expression of N-cadherin in breast cancer cells induces cell migration, invasion, and metastasis. *J Cell Biol* 2000; 148: 779-790.
- 22) NAKAJIMA S, DOI R, TOYODA E, TSUJI S, WADA M, KOIZUMI M, TULACHAN SS, ITO D, KAMI K, MORI T, KAWAGUCHI Y. N-cadherin expression and epithelial-mesenchymal transition in pancreatic carcinoma. *Clin Cancer Res* 2004; 10: 4125-4133.
- 23) GRAVDAL K, HALVORSEN OJ, HAUKAAS SA, AKSLEN LA. A switch from E-cadherin to N-cadherin expression indicates epithelial to mesenchymal transition and is of strong and independent importance for the progress of prostate cancer. *Clin Cancer Res* 2007; 13: 7003-7011.
- 24) SUYAMA K, SHAPIRO I, GUTTMAN M, HAZAN RB. A signaling pathway leading to metastasis is controlled by N-cadherin and the FGF receptor. *Cancer Cell* 2002; 2: 301-314.
- 25) TANAKA H, KONO E, TRAN CP, MIYAZAKI H, YAMASHIRO J, SHIMOMURA T, FAZLI L, WADA R, HUANG J, VESSELLA RL, AN J, HORVATH S, GLEAVE M, RETTIG MB, WAINBERG ZA, REITER RE. Monoclonal antibody targeting of N-cadherin inhibits prostate cancer growth, metastasis and castration resistance. *Nat Med* 2010; 16: 1414-1420.
- 26) ZOU CY, WANG J, SHEN JN, HUANG G, JIN S, YIN JQ, GUO QC, LI HM, LUO L, ZHANG M, ZHANG LJ. Establishment and characteristics of two syngeneic human osteosarcoma cell lines from primary tumor and skip metastases. *Acta Pharmacol Sin* 2008; 29: 325-332.
- 27) ODAGIRI H, KADOMATSU T, ENDO M, MASUDA T, MORIOKA MS, FUKUHARA S, MIYAMOTO T, KOBAYASHI E, MIYATA K, AOI J, HORIGUCHI H, NISHIMURA N, TERADA K, YAKUSHIJI T, MANABE I, MOCHIZUKI N, MIZUTA H, OIKE Y. The secreted protein ANGPTL2 promotes metastasis of osteosarcoma cells through integrin $\alpha 5\beta 1$, p38 MAPK, and matrix metalloproteinases. *Sci Signal* 2014; 7: ra7.
- 28) SKOV V, GLINTBORG D, KNUDSEN S, JENSEN T, KRUSE TA, TAN O, BRUSGAARD K, BECK-NIELSEN H, HØJLUND K. Reduced expression of nuclear-encoded genes involved in mitochondrial oxidative metabolism in skeletal muscle of insulin-resistant women with polycystic ovary syndrome. *Diabetes* 2007; 56: 2349-2355.
- 29) BUDDINGH EP, KUIJER ML, DUIM RAJ, BÜRGER H, AGELOPOULOS K, MYKLEBOST O, SERRA M, MERTENS F, HOGENDOORN PC, LANKESTER AC, CLETON-JANSEN AM. Tumor-infiltrating macrophages are associated with metastasis suppression in high-grade osteosarcoma: a rationale for treatment with macrophage activating agents. *Clin Cancer Res* 2011; 17: 2110-2119.
- 30) BORST P, JONKERS J, ROTTENBERG S. What makes tumors multidrug resistant? *Cell Cycle* 2007; 6: 2782-2787.
- 31) MCKENNA WL, ORTIZ-LONDONO CF, MATHEW TK, HOANG K, KATZMAN S, CHEN B. Mutual regulation between *Satb2* and *Fezf2* promotes subcerebral projection neuron identity in the developing cerebral cortex. *Proc Natl Acad Sci USA* 2015; 112: 11702-11707.

- 32) HAN K, ZHAO T, CHEN X, BIAN N, YANG T, MA Q, CAI C, FAN Q, ZHOU Y, MA B. microRNA-194 suppresses osteosarcoma cell proliferation and metastasis in vitro and in vivo by targeting CDH2 and IGF1R. *Int J Oncol* 2014; 45: 1437-1449.
- 33) TANG QL, XIE XB, WANG J, CHEN Q, HAN AJ, ZOU CY, YIN JQ, LIU DW, LIANG Y, ZHAO ZQ, YONG BC, ZHANG RH, FENG QS, DENG WG, ZHU XF, ZHOU BP, ZENG YX, SHEN JN, KANG T. Glycogen synthase kinase-3 β , NF- κ B signaling, and tumorigenesis of human osteosarcoma. *J Natl Cancer Inst* 2012; 104: 749-763.
- 34) ZHAO Z, WU MS, ZOU C, TANG Q, LU J, LIU D, WU Y, YIN J, XIE X, SHEN J, KANG T, WANG J. Downregulation of MCT1 inhibits tumor growth, metastasis and enhances chemotherapeutic efficacy in osteosarcoma through regulation of the NF- κ B pathway. *Cancer Lett* 2014; 342: 150-158.
- 35) LU J, SONG G, TANG Q, ZOU C, HAN F, ZHAO Z, YONG B, YIN J, XU H, XIE X, KANG T, LAM Y, YANG H, SHEN J, WANG J. IRX1 hypomethylation promotes osteosarcoma metastasis via induction of CXCL14/NF- κ B signaling. *J Clin Invest* 2015; 125: 1839-1856.
- 36) ADHIKARI AS, AGARWAL N, WOOD BM, PORRETTA C, RUIZ B, POCHAMPALLY RR, IWAKUMA T. CD117 and Stro-1 identify osteosarcoma tumor-initiating cells associated with metastasis and drug resistance. *Cancer Res* 2010; 70: 4602-4612.
- 37) LEVINGS PP, MCGARRY SV, CURRIE TP, NICKERSON DM, MCCLELLAN S, GHIVIZZANI SC, STEINDLER DA, GIBBS CP. Expression of an exogenous human Oct-4 promoter identifies tumor-initiating cells in osteosarcoma. *Cancer Res* 2009; 69: 5648-5655.
- 38) CONNER JR, HORNICK JL. SATB2 is a novel marker of osteoblastic differentiation in bone and soft tissue tumours. *Histopathology* 2013; 63: 36-49.
- 39) DAVIS JL, HORVAI AE. Special AT-rich sequence-binding protein 2 (SATB2) expression is sensitive but may not be specific for osteosarcoma as compared with other high-grade primary bone sarcomas. *Histopathology* 2016; 69: 84-90.
- 40) MACHADO I, NAVARRO S, PICCI P, LLOMBART-BOSCH A. The utility of SATB2 immunohistochemical expression in distinguishing between osteosarcomas and their malignant bone tumor mimickers, such as Ewing sarcomas and chondrosarcomas. *Pathol Res Pract* 2016; 212: 811-816.
- 41) SEONG BKA, LAU J, ADDERLEY T, KEE L, CHAUKOS D, PIENKOWSKA M, MALKIN D, THORNER P, IRWIN MS. SATB2 enhances migration and invasion in osteosarcoma by regulating genes involved in cytoskeletal organization. *Oncogene* 2015; 34: 3582-3592.
- 42) YU L, LIU S, GUO W, ZHANG C, ZHANG B, YAN H, WU Z. hTERT promoter activity identifies osteosarcoma cells with increased EMT characteristics. *Oncol Lett* 2014; 7: 239-244.
- 43) AUGUSTINE CK, YOSHIMOTO Y, GUPTA M, ZIPFEL PA, SELIM MA, FEBBO P, PENDERGAST AM, PETERS WP, TYLER DS. Targeting N-cadherin enhances antitumor activity of cytotoxic therapies in melanoma treatment. *Cancer Res* 2008; 68: 3777-3784.
- 44) JIRALERSPONG S, PALLA SL, GIORDANO SH, MERIC-BERNSTAM F, LIEDTKE C, BARNETT CM, HSU L, HUNG MC, HORTOBAGYI GN, GONZALEZ-ANGULO AM. Metformin and pathologic complete responses to neoadjuvant chemotherapy in diabetic patients with breast cancer. *J Clin Oncol* 2009; 27: 3297-3302.

Supplemental Methods

Transient and Stable Transfections

For stable cell line construction, GFP-tagged plasmids containing 3 different sh.SATB2 or SATB2 cDNAs and their corresponding control plasmids were obtained from Obio Technology (Shanghai, China) Corp. Plasmids were packaged into recombinant lentiviruses by a Lenti-PacTM HIV Expression Packaging Kit (GeneCopoeia, Rockville, MD, USA). After three rounds of infection, stable transfected cells with strong GFP expression were selected by fluorescence-activated cell sorting. Western blots were used to confirm knockdown/overexpression efficiency, and the two most effective stable knockdown cell lines were chosen for the subsequent experiments.

For transient transfection, RFP-tagged plasmids

encoding two different sh.N-cadherin constructs and the corresponding vector (Obio Technology, Shanghai, China) were transfected into U2-SATB2 cells at a density of 30%-50% confluence in six-well plates using Lipofectamine 3000 (Invitrogen, Carlsbad, CA, USA).

Immunostaining and Immunofluorescence

The paraffin-embedded OS surgical samples were sectioned at 5 μ m. The sections were then dewaxed in xylene and rehydrated in graded alcohols. Endogenous peroxidase activity was quenched by incubation with 3% hydrogen peroxide for 5 min, and antigen retrieval was performed by incubating the slides with pepsin (Dako, Glostrup, Denmark) at 37°C for 10 min. The sections were

Supplemental Table I. Biological Process (GO) analysis results of 21 SATB2 target genes.

#pathway ID	Pathway description	Observed gene	False discovery rate	Matching proteins in your network (IDs)	Matching proteins in your network (labels)
GO.0031214	Biomaterial tissue development	4	0.0143	ENSP00000339824 ENSP00000340935 ENSP00000368516 ENSP00000372059	DMP1 FGFR3 IFITM5 LGR4
GO.0001503	Ossification	5	0.0336	ENSP00000260926 ENSP00000339824 ENSP00000340935 ENSP00000368516 ENSP00000372059	DMP1 FGFR3 IFITM5 LGR4 SATB2
GO.0030282	Bone mineralization	3	0.0442	ENSP00000339824 ENSP00000368516 ENSP00000372059	FGFR3 IFITM5 LGR4

incubated with antibody against SATB2 (1:200, Abcam, Cambridge, MA, USA) at 4°C overnight. For immunohistochemistry, primary antibodies were detected using the Dako EnVision Kit (Dako, Glostrup, Denmark) according to the manufacturer's protocol. The staining intensity of SATB2 was evaluated based on the percentage of positive tumor cells: 0, no staining; 1+, <5%; 2+, 5-25%; 3+, 26-50%; 4+, 51-75%; and 5+, 76-100%. The staining intensity was graded as weak (0, 1+, 2+ and 3+) or strong (4+ and 5+).

For immunofluorescence, OS cells were incubated with SATB2 antibody (1:100, Abcam, Cambridge, MA, USA). A secondary goat anti-rabbit IgG H&L antibody (Alexa Fluor® 555, Abcam, Cambridge, MA, USA) was used, and the nuclei were counterstained with DAPI (Sigma-Aldrich, St. Louis, MA, USA). Immunofluorescence was detected using a Zeiss LSM 780 confocal microscope (Oberkochen, Germany).

Bioinformatics Analysis

The gene expression profiles of OS biopsy (GSE14827) and normal skeletal muscle (GSE13205) samples were performed using an Affymetrix Human Genome U133 Plus 2.0 Array. All of the microarray data were normalized using the GCRMA package version 2.22.0 in an R 2.12.0 environment.

For the SATB2 target gene screen, a SATB2 ChIP-seq dataset (SRX1028899) was analyzed using the edgeR package 3.3, and genes with scores

greater than 0 were chosen. To identify genes co-expressed with SATB2, we analyzed the mRNA expression intensities of SATB2 and the other 48,701 genes in the OS biopsy tissue dataset GSE21257 (n=53) using Pearson correlation. After we compared the correlation coefficient scores, genes with scores >0.5 were selected. After combining the ChIP-seq and co-expression results, these genes were positively associated in the SATB2 ChIP-seq dataset, and those that shared the same expression trend were selected as candidate SATB2-targeted genes in OS. Biological Process (GO) analyses were performed in <http://www.string-db.org/>.

For the survival analyses, gene expression data from GSE21257 were clustered into groups using the median, and Kaplan-Meier analyses were performed. Significance for these plots was determined using the log-rank test.

Supplemental Table II. Sequences of the primers used for PCR are listed below.

Primer	Sequence (5' to 3')
SATB2-F	GCAGTTGGACGGCTCTCTT
SATB2-R	CACCTCCCAGCTTGATTATTC
SOX2-F	GCCGAGTGGAACTTTTGTCG
SOX2-R	GGCAGCGTGTACTTATCCTTCT
OCT3/4-F	CCTGAAGCAGAAGAGGA TCACC
OCT3/4-R	AAAGCGGCAGA TGGTCGTTTGG
CD133-F	CACTACCAAGGACAAGGCGTTC
CD133-R	CAACGCCTCTTTGGTCTCCTTG